Proceedings of the
Annual Stability Conference
Structural Stability Research Council
St. Louis, Missouri, April 2-5, 2019

Modal buckling analysis of trapezoidal sheeting

Sandor Adany[1], Qadier Tayseer Aldalaien[2]

Abstract
In this paper the linear buckling of simple trapezoidal sheet panels is discussed, in the light of the mechanics-based global-distortional-local classification. The calculations are performed by using the constrained finite element method, which can readily handle trapezoidal sheets and which can easily and objectively separate the global, distortional and local buckling of trapezoidal sheeting. A few demonstrative examples are presented. The examples imitate simple elementary cases, such as simply supported rectangular plates subjected to uni-directional uniform compression or pure shear. The examples prove that the global-distortional-local classification of deformations can meaningfully be applied to understand the complex buckling behavior of trapezoidal sheets.

1. Introduction

Trapezoidal sheeting is employed in various structural engineering applications. The primary loading is mostly perpendicular to the plane of the sheeting, but in many cases the sheeting is also subjected to in-plane actions, most typically when the sheeting is designed to contribute to the global rigidity of the structure. Due to the slender nature of the sheeting, buckling is important, especially if in-plane actions are present. Though in the case of thin-walled beam/column members it is usual to classify the buckling modes as global, distortional and local, similar classification has not rigorously been applied for trapezoidal sheeting so far. Even if in some literature global and local buckling of trapezoidal sheeting is discussed, see e.g., Dou et al (2018), the underlying phenomena are sometimes mechanically different from those described as global or local buckling of beam/column members, whilst distortional buckling of sheeting is usually not discussed. In the actual paper it is shown that the mechanical criteria behind the global-distortional-local classification of beam/column members can be used to trapezoidal sheeting, too, so that any pure buckling mode or any combination of pure buckling modes can be calculated for various loads and supports. In the paper the linear buckling of simple trapezoidal sheet panels is discussed in the light of the mechanics-based global-distortional-local classification. The calculations are performed by using the recently developed constrained finite element method, see Ádány (2018) and Ádány et al. (2018), which can readily handle trapezoidal sheets and which can easily and objectively separate the global, distortional and local buckling of

[1] Assiociate Professor, Budapest University of Technology and Economics, <sadany@epito.bme.hu>
[2] Graduate Student, Budapest University of Technology and Economics, <Qadier.aldalaien@google.com>

trapezoidal sheeting. Only a few cases are considered. The examples are slightly theoretical, since the support conditions and applied loading do not try to correspond to a certain application, but rather try to imitate simple elementary cases, such as simply supported rectangular plates subjected to uni-directional uniform compression or pure shear.

2. The constrained finite element method

The constrained finite element method (cFEM) is essentially a shell finite element method, but the finite element is developed so that modal decomposition would be possible. Separation of the behaviour modes is realized by applying mechanical constraints. In order to maintain constraining ability, the longitudinal shape functions are specially selected, but the shell elements can be used as any regular flat shell element. When a member is constrained into a deformation mode (e.g., to global mode), it is enforced to deform in accordance with some mechanical criteria, characterizing for the intended deformation mode. The criteria can be expressed by **R** constraint matrices. The application of the constraint matrix enforces to fulfil certain relationship between various nodal degrees of freedom, specific to the given 'M' deformation space. This automatically means a reduction of the effective degrees of freedom. Mathematically, the **d** displacement vector is expressed as follows:

$$\mathbf{d} = \mathbf{R}_\mathbf{M}\mathbf{d}_\mathbf{M} \tag{1}$$

where $\mathbf{R}_\mathbf{M}$ is the constraint matrix to the M space, and $\mathbf{d}_\mathbf{M}$ is the reduced displacement vector. Since the $\mathbf{d}_\mathbf{M}$ reduced displacement vector has fewer elements than that of the original **d** vector, the elements of $\mathbf{d}_\mathbf{M}$ vector cannot (typically) be interpreted as nodal displacements anymore. The column vectors of the constraint matrix can also be viewed as the *basis vectors* of the displacement field that is represented by the constraint matrix, that is, in Eq. (1) the **d** displacement vector is expressed as a linear combination of base vectors, where the combination factors are the entries of the $\mathbf{d}_\mathbf{M}$ vector.

An important feature of the finite element analysis by cFEM is that transverse and longitudinal directions are strictly distinguished. When deformations are constrained or decomposed, these are the transverse cross-section deformations that are manipulated, practically independently of the employed longitudinal shape functions. Moreover, cFEM modal decomposition or constraints can be applied to either the whole member at once, or to any of its bands (where *band* is a small section of the member with one single shell element longitudinally, see Fig. 1). It is found to be more convenient to complete the constraining band by band, so this approach is followed here.

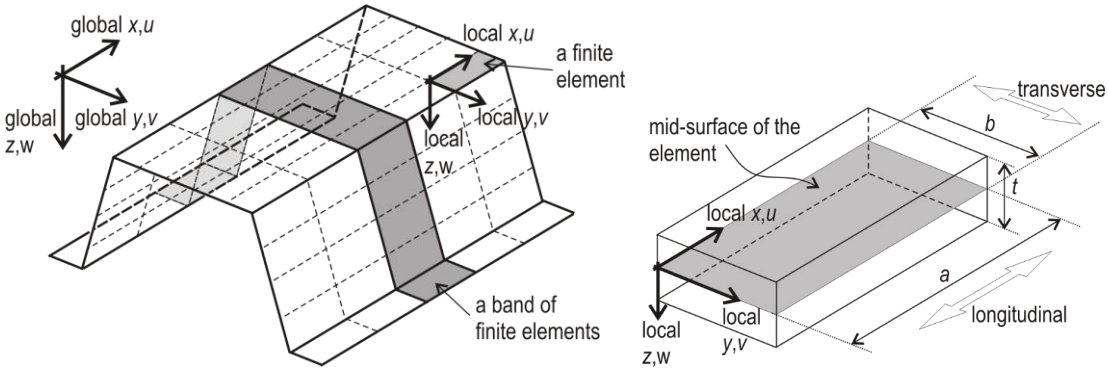

Figure 1: cFEM discretization and basic terminology.

Since cross-section constraints are essentially independent of the longitudinal displacement distributions, various longitudinal shape functions can be used. In classic finite element analysis Lagrange and Hermite polynomials are used, which are employed also in cFEM whenever buckling analyses are performed. (Note, in other cases, notably when cFEM is used for modal identification, Fourier-like longitudinal functions are found to be more convenient, but this feature of cFEM is not utilized here.)

In the case of linear buckling analysis, when the problem is formulated as a generalized eigen-value problem, the equation to solve is:

$$\mathbf{K_e \Phi} - \mathbf{\Lambda K_g \Phi} = \mathbf{0} \tag{2}$$

where $\mathbf{K_e}$ and $\mathbf{K_g}$ are the global elastic and geometric stiffness matrices, and

$$\mathbf{\Lambda} = \text{diag} < \lambda_1\, \lambda_2\, \lambda_3 \ldots \lambda_{nDOF} > \qquad \text{and} \quad \mathbf{\Phi} = [\boldsymbol{\phi_1}\, \boldsymbol{\phi_2}\, \boldsymbol{\phi_3} \ldots \boldsymbol{\phi_{nDOF}}] \tag{3}$$

where λ_i is the critical load multiplier and $\boldsymbol{\phi_i}$ is the associated buckling shape, and *nDOF* denotes the number of degrees of freedom. When the constraints are enforced, the displacement vector is expressed by modal coordinates, see Eq. (1). This equation can also be applied to any buckling shape $\boldsymbol{\phi}$, since the buckling shape itself is a displacement vector. Therefore:

$$\boldsymbol{\phi} = \mathbf{R_M}\, \boldsymbol{\phi_M} \tag{4}$$

which is another generalized eigen-value problem, given in the reduced M deformation space, where $\mathbf{K_{eM}}$ and $\mathbf{K_{gM}}$ can be regarded as the modal version of the elastic and geometric stiffness matrix, respectively. Solving the above equation leads to the modal eigen-vectors $\boldsymbol{\phi_M}$, from which the buckled shapes $\boldsymbol{\phi}$ can be back-calculated by using Eq. (4).

3. Deformation modes of trapezoidal sheets

In Fig. 2 some characteristic deformation modes are shown for trapezoidal corrugated sheets. The deformation modes can be interpreted as the modes of a beam or column member, where the cross-section has a zig-zag shape, but the cross-section is constant in the longitudinal direction. As always, the deformation modes are independent of the supports, defined solely by the member (i.e., corrugated sheet) geometry. In Fig. 2 the deformation modes are shown by axonometric figures, by using a single half-sine-wave for the longitudinal distribution, but it is to emphasize that the longitudinal displacement distribution has no real effect on the displacement modes, so the half-sine-waves are used here just for illustration.

The nature of the deformation modes is primarily determined by the topology of the cross-section, i.e., the shape ad number of troughs, though the exact shapes and the order of the deformation modes are dependent on the geometric proportions (and in some cases on the discretization, too). Thus, the deformation modes presented here can be regarded as qualitatively representative for trapezoidal sheets. Only minor-axis and major-axis global bending (GB1 and GB2), global torsion (GT), distortional (D), and a primary local (LP) modes are shown. More information on the deformation modes in general can be found in Ádány (2018) and Ádány et al. (2018).

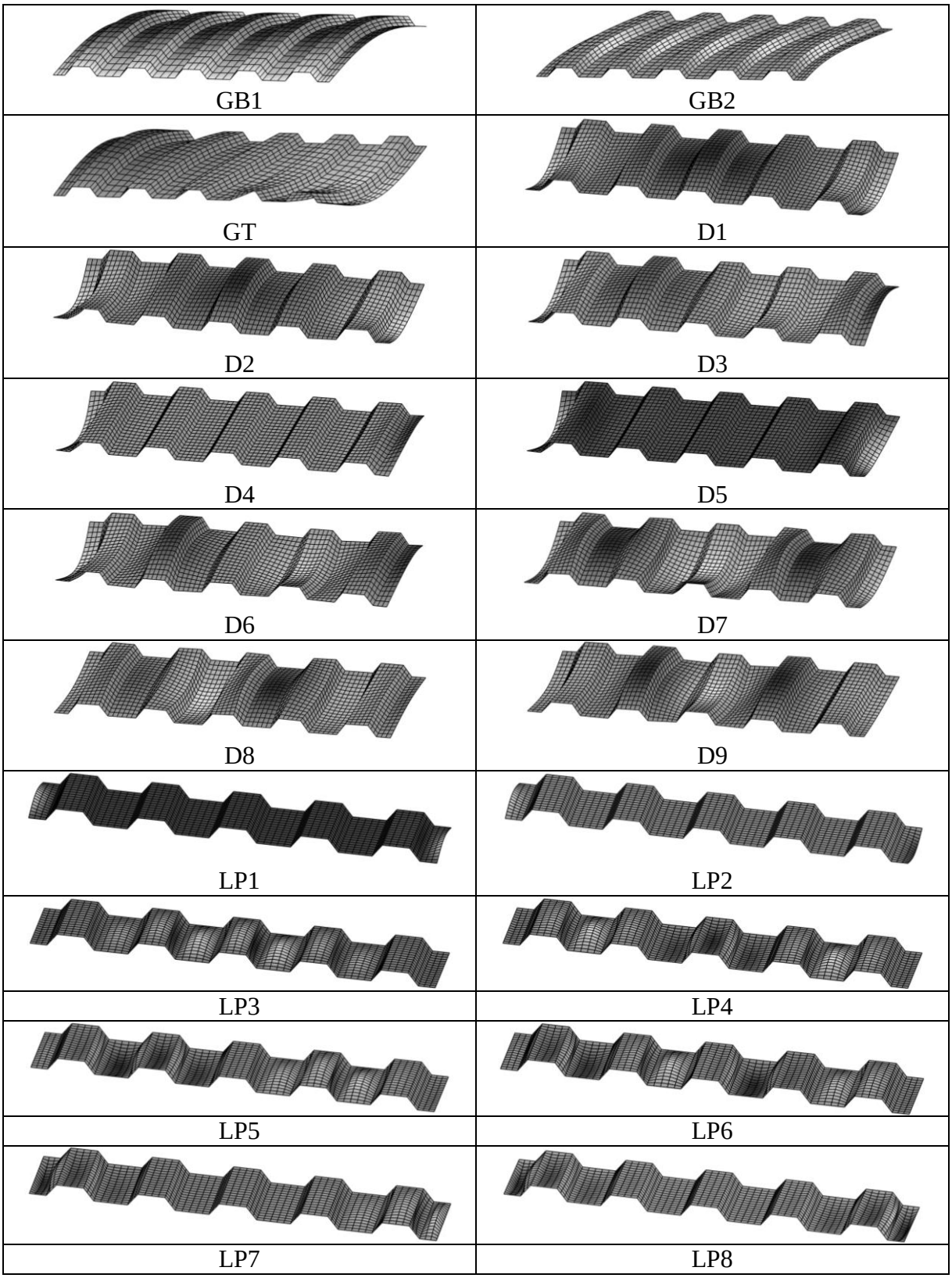

Figure 2: Deformation modes of trapezoidal sheets, samples.

Fig. 2 shows the case of a plate with 5 corrugations. GB1, GB2 and GT are classic global modes with rigid-body cross-section displacements. For the actual geometry the number of D modes is 18, but only the first 9 D modes are shown. D modes are characterized by cross-section distortion which can be observed at the mid-length of the member in Fig. 2. It can be observed that most of D modes are characterized by a certain number of half-waves in the transverse direction, e.g., D1 and D2 have 2 transverse half-waves (note, D1 and D2 look very similar, but still different), D3 and D6 have 3 transverse half-waves (note again, D3 and D6 look very similar, but still different), etc. For the actual geometry the number of LP modes is 24, but only the first 8 are shown. As expected, in the case of local deformation modes the intersection lines of the connecting plate elements remain straight.

4. Buckling of trapezoidal sheets subjected to pure compression

Three examples are presented here to illustrate the modal buckling behaviour of trapezoidal sheets if subjected to pure axial compression. The selected sheet geometry is as follows: the length is 600 mm, the sheet depth is 20 mm, the width of the lower flanges is 50 mm, the width of the upper flanges is 40 mm, the total width of one single corrugation is 120 mm, while the thickness is 1.5 mm. The only difference between the examples is the number of corrugations. In Example #1 the sheet is consisted of 3 corrugations, hence the total width is 360 mm, in Example #2 there are 5 corrugations (total width: 600 mm), while in Example #3 there are 7 corrugations (total width is 840 mm).

The material is steel-like, with E=210000 MPa, but the Poisson's ratio is set to zero (in order to avoid the potential artificial stiffening effect of the constraining, which is discussed e.g. in Ádány (2012). The load is a longitudinal compression, uniformly distributed over the end cross-sections, its intensity is 1 N/mm^2.

The sheet is supported along all its 4 edges by simple supports. For the longitudinal (straight) edges the simple support means that translations in Y and Z are restrained. For the transverse (zig-zag) edges the simple support means that translations in the local z directions are restrained (which corresponds to a locally and globally pinned support if the sheeting panel is interpreted as a beam/column member).

Linear buckling analyses have been performed by using various constraints, and the first few buckled shapes and corresponding critical values are determined. The following constraints are applied: local modes only (L), distortional modes only (D), global and distortional modes (G+D), global, distortional and local modes (G+D+L), and also analyses without any constraints. It is to note that solution in G only does not practically exist, since GB1, GB2 and GT deformations all contradict to the applied boundary conditions. The results are summarized in Figs. 3, 4 and 5, for Example #1, #2 and #3, respectively. For all the constraining options the first two buckling modes are given.

As far as pure L buckling is concerned, the buckled shapes consist of various numbers of half-waves (longitudinally) in the wider (i.e., lower) flanges. The critical stress values are marginally affected by the number of corrugations, the lowest pure L critical stresses being around 845-850 N/mm^2.

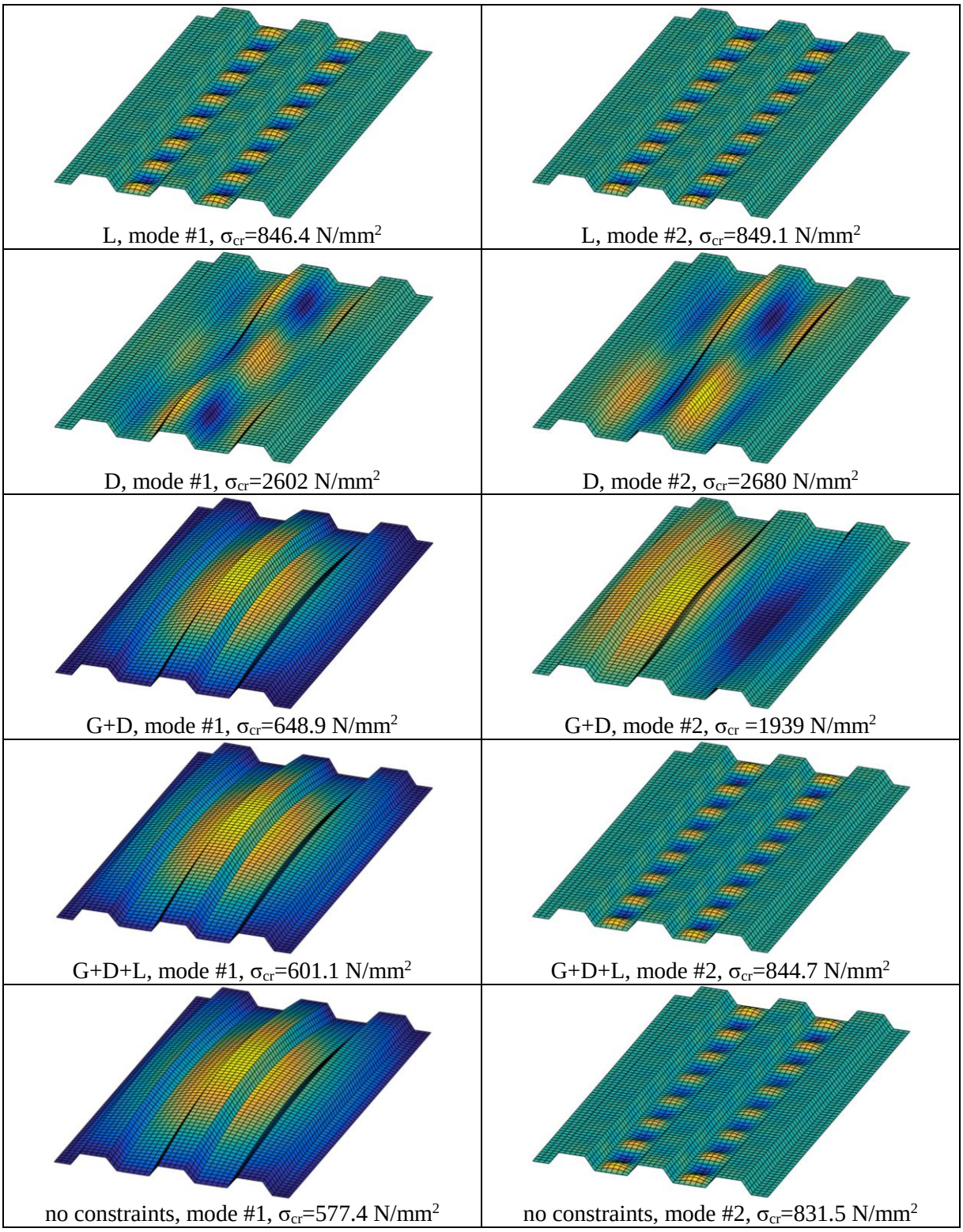

Figure 3: Example #1, buckling results by enforcing various constraints

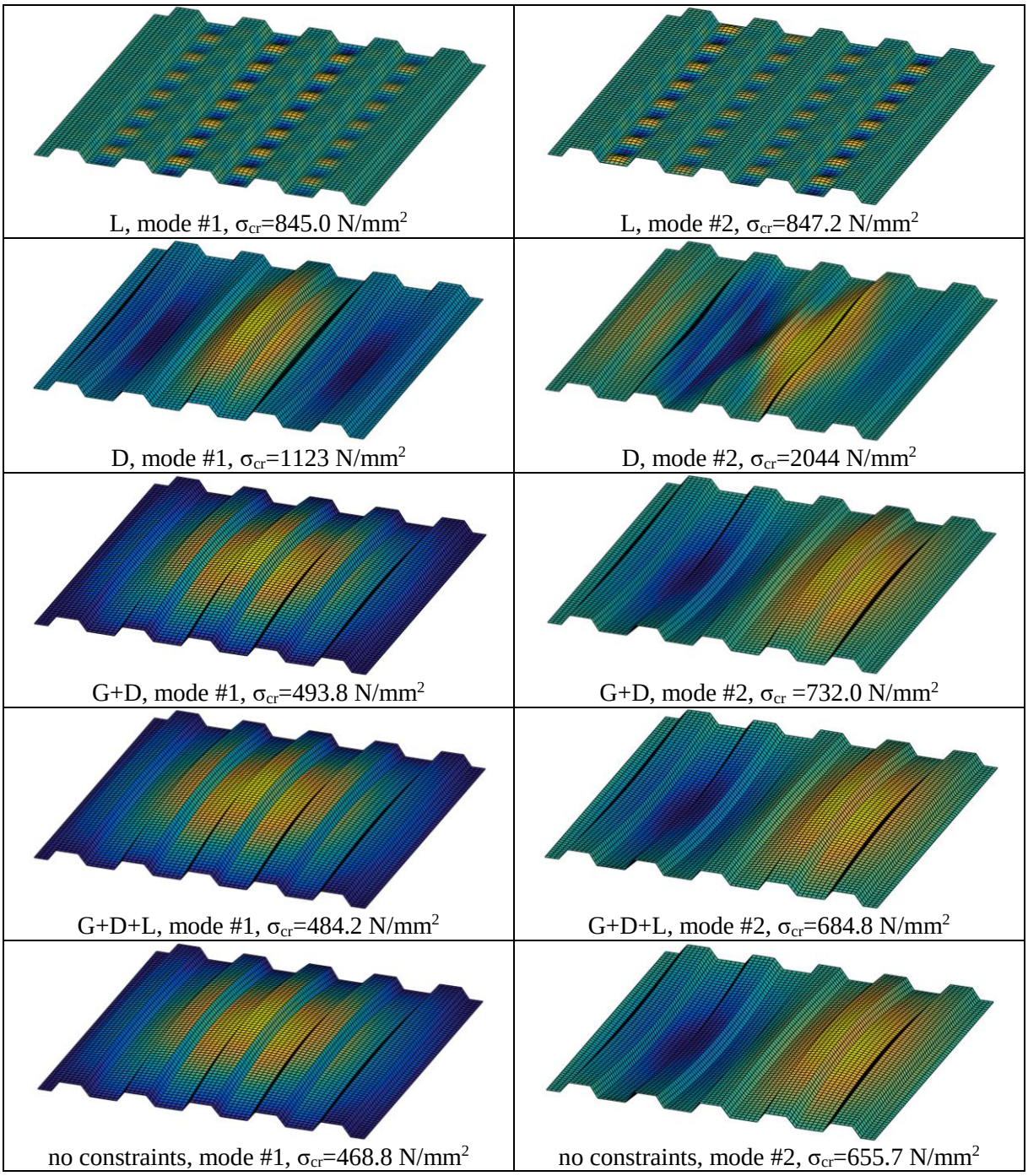

Figure 4: Example #2, buckling results by enforcing various constraints

Pure distortional buckling exists. The longitudinal wavelength and the number of transverse waves are depending on the sheet geometry, especially on the corrugation number. For example, in the case of three corrugations there are 2 or 3 half-waves longitudinally in the first two pure distortional buckling modes, but for larger number of corrugations there is only one half-wave longitudinally. The value of the lowest pure D critical stress is strongly dependent on the number of corrugations. In the case of 3 corrugations the pure D critical stress is rather high (approx.

2600 N/mm^2), but this critical value is rapidly decreasing as the number of corrugations is increasing (e.g., approx. 700 N/mm^2 for 7 corrugations).

Even though the G deformation modes contradict to the considered boundary conditions, G deformation modes have important role in the buckling behavior. As soon as G deformation modes are added to the D deformations, the lowest buckled shapes as well as the corresponding critical values become fairly similar to those from the 'no constraints' solutions. This also means that the importance of the L and O other (i.e., in-plane shear and transverse extension) deformations in the 'no constraints' solutions is relatively small, at least in these examples. It can also be observed that the importance of L and O modes become smaller and smaller as the number of corrugations is increasing.

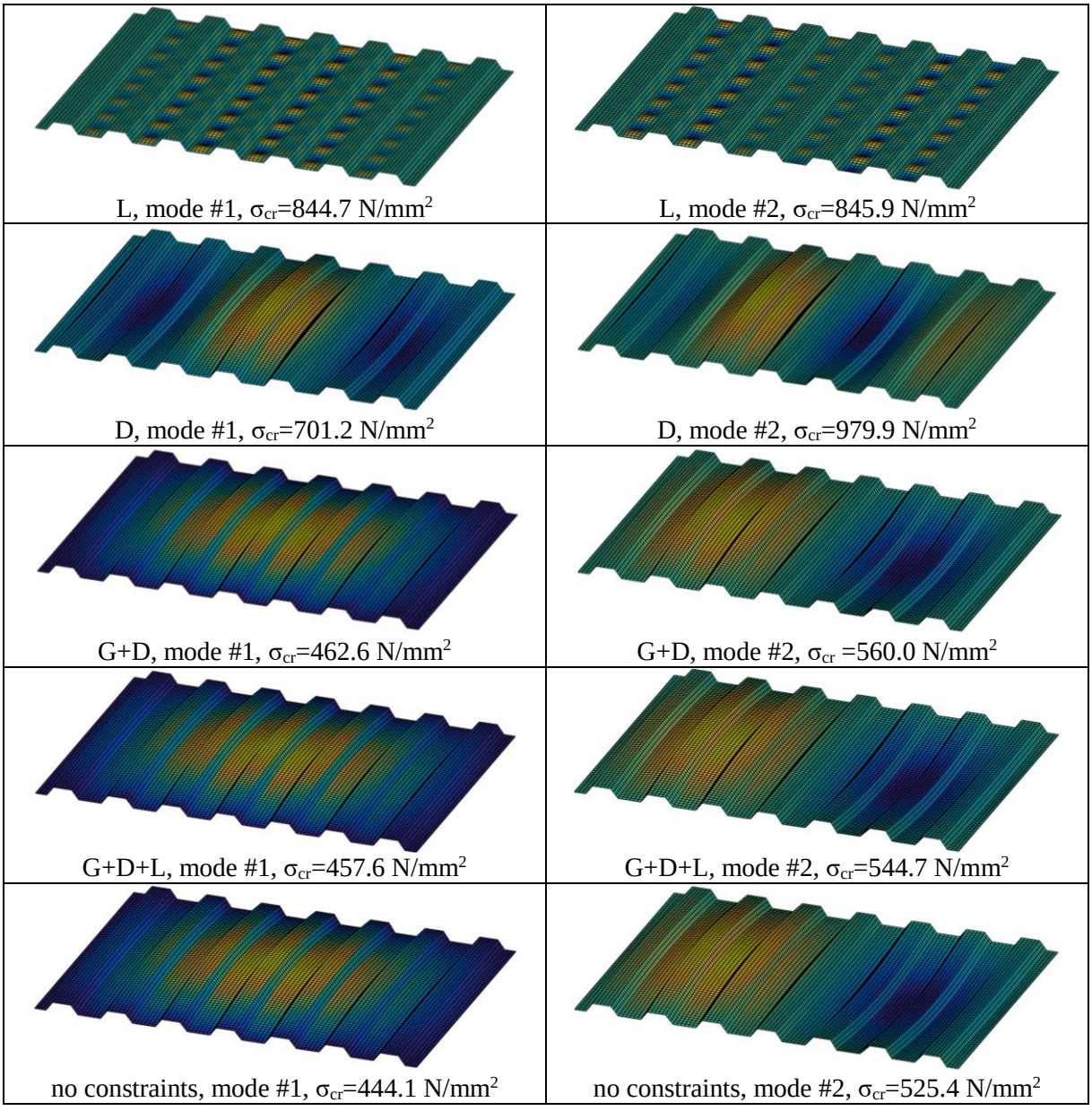

Figure 5: Example #3, buckling results by enforcing various constraints

5. Buckling of trapezoidal sheeting subjected to pure shear

Three examples, i.e., Examples #4, #5 and #6, are presented here to illustrate the modal buckling behaviour of trapezoidal sheets if subjected to pure shear.

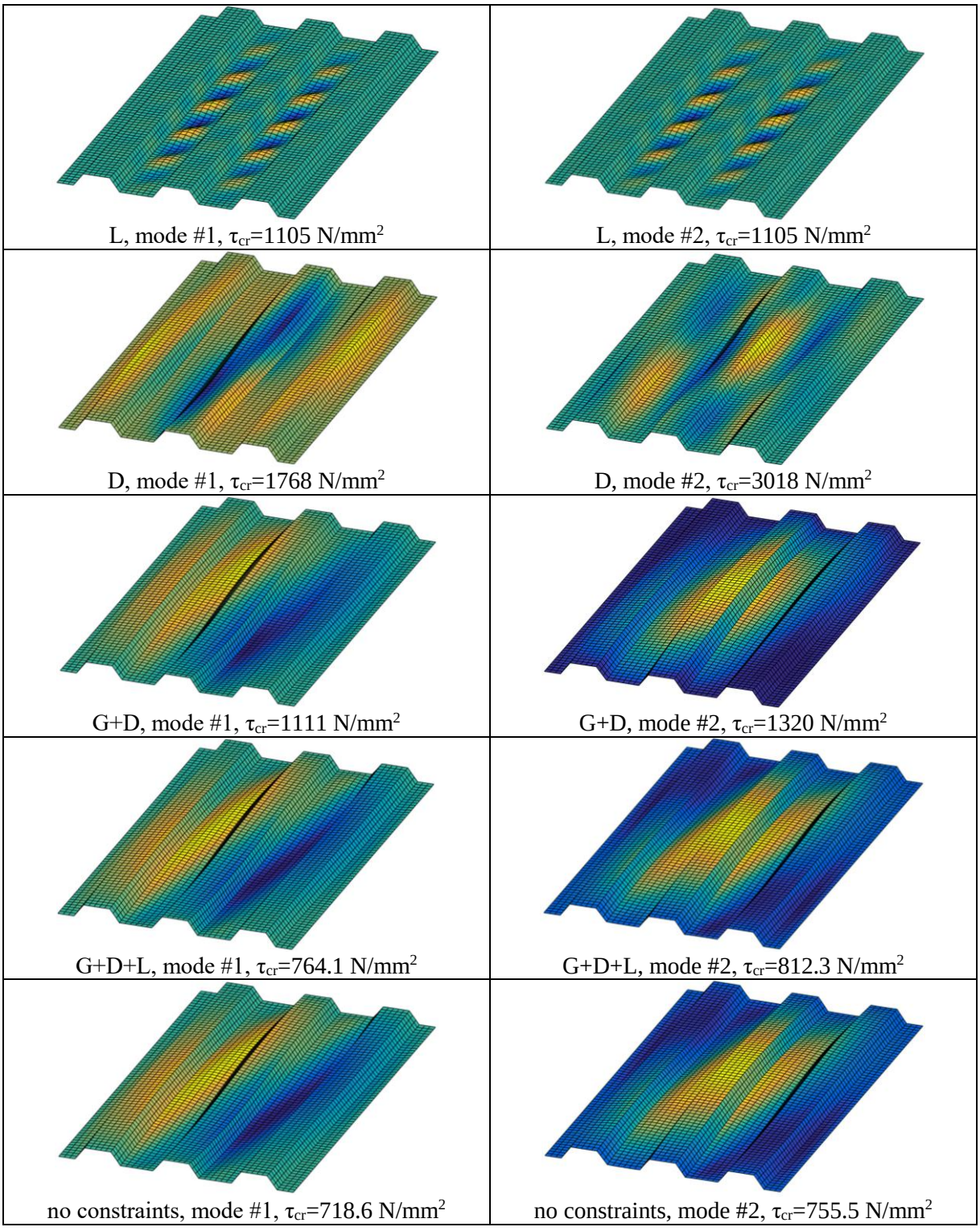

Figure 6: Example #4, buckling results by enforcing various constraints

The examples are essentially identical to the previous ones (e.g., same geometries, same supports, same material), the only difference is the loading. Pure shear loading is applied, realized by distributed loading, applied to all 4 edges, always parallel with the actual edge. The load intensity is defined so that the shear stress in the whole sheet would be equal to 1 N/mm^2. Linear buckling analyses have been performed by using the same constraining options as in the previous Section. The results are summarized in Figs. 6, 7 and 8, for Example #4, #5 and #6, respectively. For all the constraining options the first two buckling modes are given.

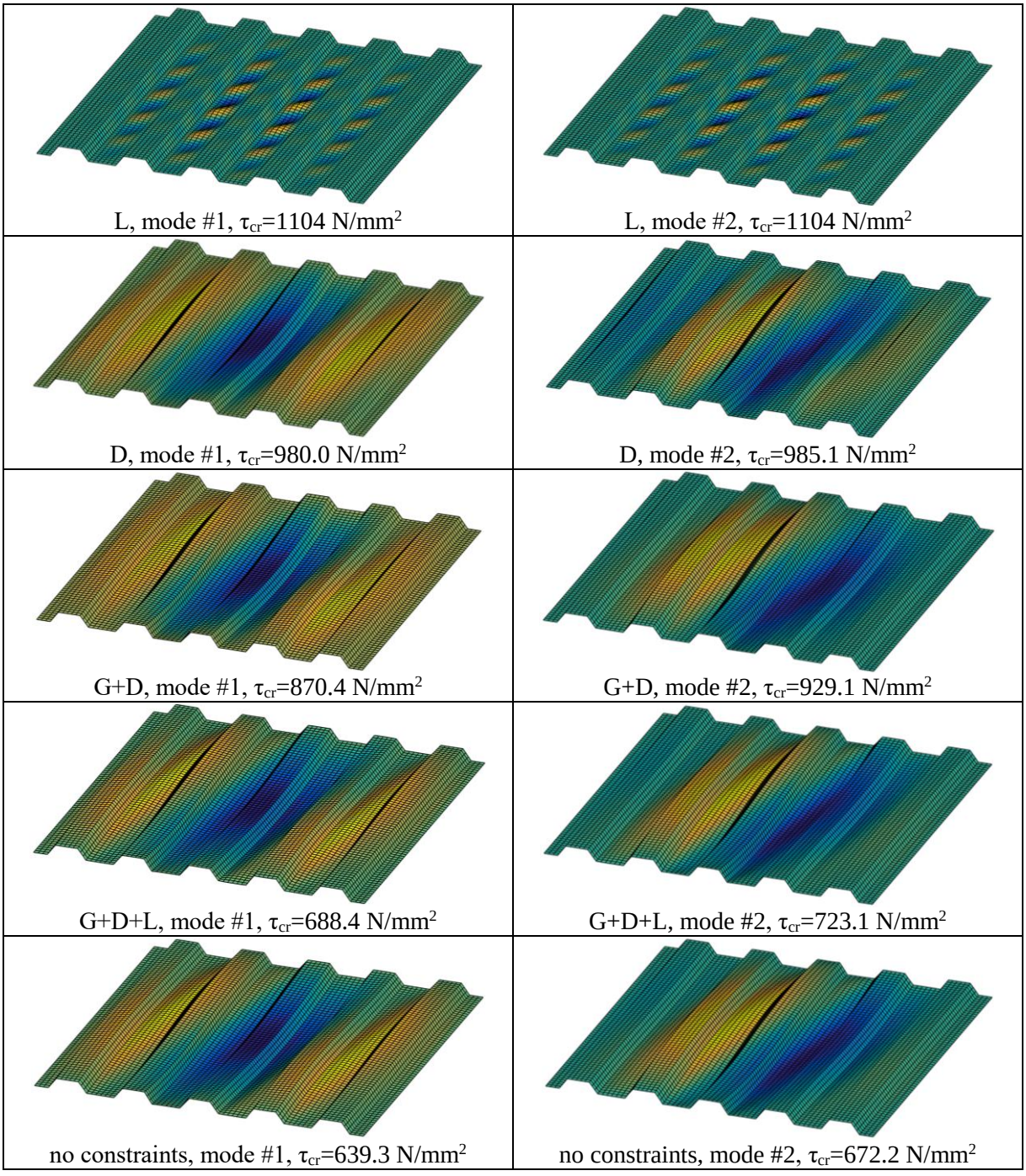

Figure 7: Example #5, buckling results by enforcing various constraints

In general, the tendencies and observations are similar to those from the previous examples. For example, L buckling takes place in the wider (i.e., lower) flanges, but now the buckled shapes show the classic shear plate buckling patterns. The critical stress values are marginally affected by the number of corrugations, the lowest pure L critical stresses being around 1105 N/mm^2.

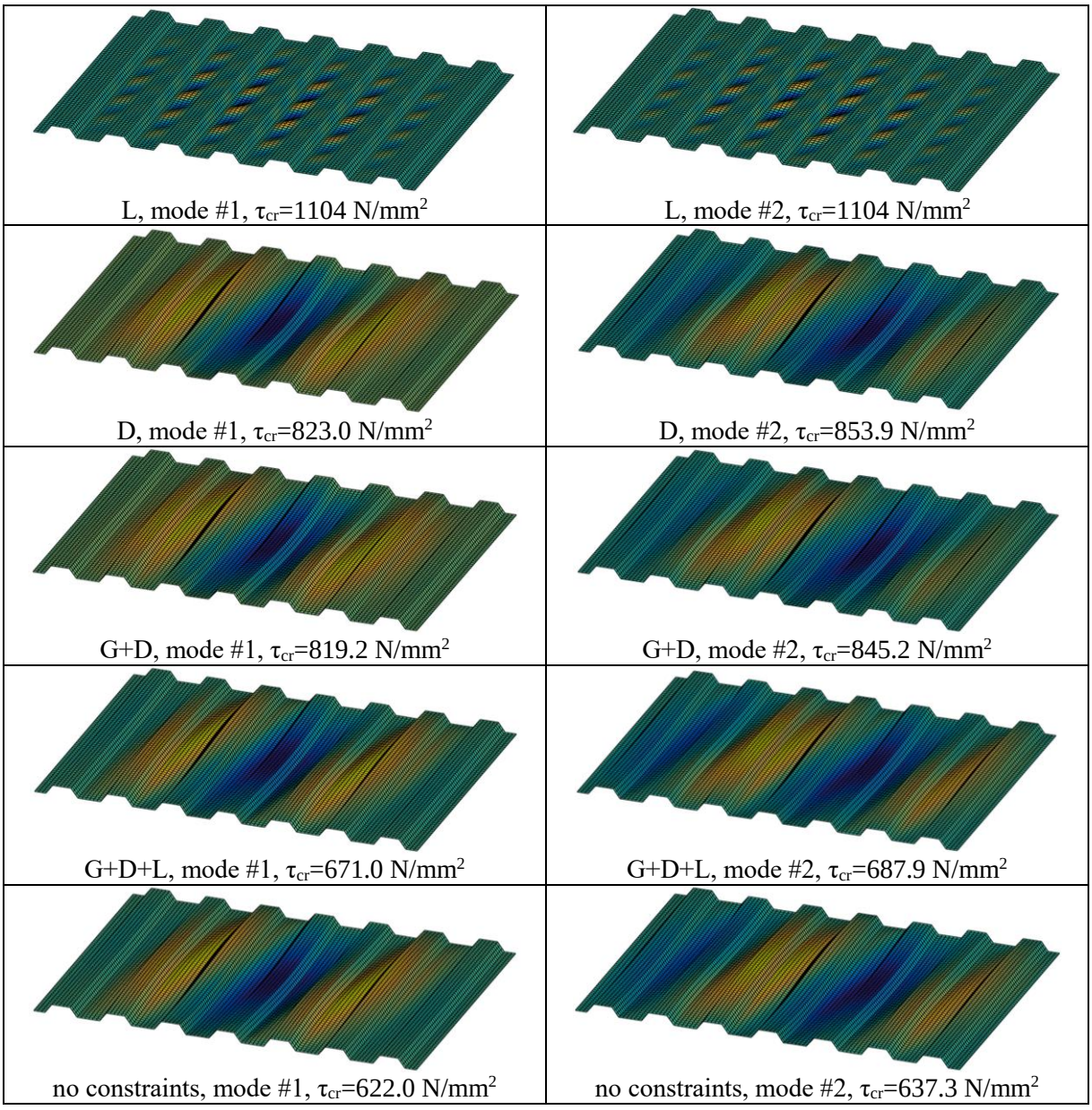

Figure 8: Example #6, buckling results by enforcing various constraints

Pure distortional buckling exists also in the case of shear loading. Similarly to the pure compression case, the value of the lowest pure D critical stress is strongly dependent on the number of corrugations: in the case of 3 corrugations the pure D critical stress is rather high (approx. 1770 N/mm^2), but this critical value is rapidly decreasing as the number of corrugations is increasing (e.g., approx. 820 N/mm^2 for 7 corrugations). Unlike in the case of pure compression, however, the buckling pattern is hardly affected by the number of corrugations.

G deformations have important role. It is to observe that the buckled shapes from the G+D options are visually identical to those from the 'no constraints' solutions. However, the critical values from the G+D and from the 'no constraints' solutions are fairly different. This indicates the importance of L and O deformations. By looking at the G+D+L critical values, however, it turns out that L deformation have pronounced role in these actual examples.

6. Conclusions

In this paper the constrained finite element method has been applied to study the buckling behavior of trapezoidal sheets. Since the method interprets the behavior as the superposition of global, distortional, local and other deformation modes, it makes possible to understand the complex buckling behavior of trapezoidal sheets as a superposition of modal behavior components. In the paper a few elementary examples are shown and discussed. Based on the results, the following conclusions can be drawn:

- The constrained finite element method is applicable not only to beam-like thin-walled members, but also to plates, including trapezoidal sheets.
- The G+D+L classification of the deformations can readily and meaningfully be applied to trapezoidal sheets. Though it is not typical to discuss distortional buckling of simple trapezoidal sheets, D deformations exist. Pure D buckling exists, too. If the corrugation number is large enough, pure D critical value might be reasonably close to the regular finite element solution (without constraints), which suggests that D deformations are dominant.
- Even if the boundary conditions do not allow pure G deformations (that is, they do not allow pure G buckling), G deformations are crucially important in the behavior.
- Pure L, or pure D buckling exist for various loading situation, including pure shear loading.

Though it is not discussed in this paper, the results show that the support conditions have important effect on the behavior. Also, the exact realization of the loading is an important factor to consider. Most surely the sheet geometry has important effect. All these questions should be studied in the future.

Acknowledgments

The presented work was conducted with the financial support of the K119440 project of the Hungarian National Research, Development and Innovation Office.

References

Ádány S. (2012), Global Buckling of Thin-Walled Columns: Analytical Solutions based on Shell Model, *Thin-Walled Structures*, Vol 55, 2012., pp 64-75.

Ádány S. (2018), Constrained shell Finite Element Method for thin-walled members, Part1: constraints for a single band of finite elements, *Thin-Walled Structures*, Vol 128, July 2018, pp. 43-55.

Ádány S., Visy D., Nagy R. (2018), Constrained shell Finite Element Method, Part 2: application to linear buckling analysis of thin-walled members, *Thin-Walled Structures*, Vol 128, July 2018, pp. 56-70.

Dou C., Pi Y.-L., Gao W. (2018), Shear resistance and post-buckling behavior of corrugated panels in steel plate shear walls, *Thin-Walled Structures*, Vol 131, 2018, pp. 816-826.